Redox-linked Protonation State Changes in Cytochrome bc_1 Identified by Poisson-Boltzmann Electrostatics Calculations

Astrid R. Klingen[a], Hildur Palsdottir[b], Carola Hunte[b] and G. Matthias Ullmann[a]

[a]Structural Biology/Bioinformatics Group, University of Bayreuth, Germany;
[b]Department of Molecular Membrane Biology, Max Planck Institute of Biophysics, Frankfurt am Main, Germany

November 29, 2006

Submitted to Biochim. Biophys. Acta

— Supplementary Material —

1. Calculation of partial charges for cofactors of cytochrome bc_1

In Poisson-Boltzmann calculations, every atom needs to be assigned a certain partial charge. For the protein residues in cytochrome bc_1, standard partial charges from the CHARMM22 parameter set [1] were used. Charges for the detergent undecylmaltopyranoside were derived from the standard CHARMM partial charges for glucose. Charges for all other compounds were obtained from density functional theory (DFT) calculations. The resulting partial charges of non-protein compounds of cytochrome bc_1 in all considered protonation and redox forms are listed in Tables 1.2 to 1.14. The atom nomenclature used in these tables corresponds to the atom names in the PDB-deposited cytochrome bc_1 structures 1P84 [2] and 1KB9 [3]. All charges are given as fractions of the elementary charge e.

The calculation of partial charges for the Rieske cluster [4, 5] and coenzyme Q [6] have been reported in previous publications from our group. New DFT calculations were performed with the ADF programme suite [7], using functionals VWN [8] and PW91 [9]. Input coordinates for the new DFT calculations were derived from the crystal structures of cytochrome bc_1 from *Saccharomyces cerevisiae*, unless stated otherwise in the legends of the respective tables. Partial charges were derived from the DFT calculation results by a CHELPG-based algorithm [10] combined with singular value decomposition [11]. Atom radii used in the fitting procedure are given in Table 1.1. These correspond to the radii published by Bondi [12] except for the radius of hydrogen, where we use 1.0 Å instead of Bondi's 1.2 Å.

Table 1.1. Atom radii in Å used in the fitting of atomic partial charges to the electrostatic potentials obtained from the DFT calculations.

atom type	radius
C	1.7
H	1.0
N	1.55
O	1.5
S	1.8
Fe	1.4
P	2.0

Table 1.2. Partial charges in e for the b-type haem groups in their oxidised and reduced form. Input coordinates for the DFT calculations were derived from the high-resolution structure of a small prokaryotic b-type cytochrome [13].

atom		partial charge	
		ox	red
haem	FE	0.635	0.486
	CHA	−0.378	−0.349
	CHB	−0.198	−0.196
	CHC	−0.097	−0.102
	CHD	−0.251	−0.266
	NA	−0.111	−0.016
	C1A	0.089	0.001
	C2A	−0.170	−0.129
	C3A	−0.070	−0.086
	C4A	0.049	−0.031
	CMA	−0.251	−0.188
	CAA	0.151	0.075
	NB	0.003	0.069
	C1B	−0.039	−0.093
	C2B	0.030	0.049
	C3B	0.009	−0.047
	C4B	−0.154	−0.186
	CMB	−0.308	−0.272
	CAB	−0.094	−0.057
	CBB	−0.456	−0.532
	NC	−0.106	−0.040
	C1C	−0.158	−0.207
	C2C	0.116	0.131
	C3C	−0.157	−0.203
	C4C	0.152	0.124
	CMC	−0.313	−0.289
	CAC	−0.087	−0.043
	CBC	−0.487	−0.554
	ND	−0.207	−0.169
	C1D	0.067	0.034
	C2D	0.031	0.010
	C3D	−0.266	−0.239
	C4D	0.083	0.024
	CMD	−0.336	−0.305
	CAD	0.247	0.181
	HMC1	0.128	0.106
	HMC2	0.128	0.106
	HMC3	0.128	0.106
	HMB1	0.124	0.099
	HMB2	0.125	0.099
	HMB3	0.125	0.098
	HAA2	0.020	0.022
	HAA1	0.020	0.022
haem	HMA1	0.110	0.081
	HMA2	0.110	0.081
	HMA3	0.120	0.082
	HAD1	−0.007	−0.009
	HAD2	−0.007	−0.009
	HMD1	0.138	0.114
	HMD2	0.137	0.114
	HMD3	0.137	0.114
	HC	0.176	0.173
	HAC	0.153	0.135
	HBC1	0.244	0.227
	HBC2	0.224	0.227
	HBB1	0.218	0.213
	HBB2	0.218	0.213
	HAB	0.149	0.137
	HA	0.272	0.264
	HD	0.170	0.169
	HB	0.198	0.197
1st ligand His	CB	0.143	0.076
	CG	0.022	0.070
	ND1	−0.298	−0.349
	CD2	−0.390	−0.420
	CE1	−0.064	−0.070
	NE2	0.002	0.003
	HB1	0.029	0.028
	HB2	0.029	0.028
	HE1	0.154	0.148
	HD2	0.223	0.221
	HD1	0.377	0.367
2nd ligand His	CB	0.131	0.068
	CG	0.014	0.041
	ND1	−0.284	−0.310
	CD2	−0.374	−0.403
	CE1	−0.109	−0.137
	NE2	0.053	0.065
	HB1	0.029	0.031
	HB2	0.029	0.031
	HD2	0.220	0.224
	HE1	0.162	0.158
	HD1	0.374	0.360

Table 1.2 continued

Table 1.3. Partial charges in e for haem c_1 in its oxidised and reduced form. Input coordinates for the DFT calculations were derived from the high-resolution structure of cytochrome c from horse mitochondria [14].

atom		partial charge	
		ox	red
haem	FE	0.376	0.339
	NA	0.150	0.150
	NB	0.138	0.180
	NC	0.057	0.057
	ND	0.127	0.162
	C1A	−0.162	−0.192
	C2A	−0.182	−0.151
	C3A	0.001	−0.084
	C4A	−0.053	−0.030
	C1B	0.012	0.029
	C2B	−0.054	−0.097
	C3B	−0.037	−0.046
	C4B	−0.156	−0.199
	C1C	0.017	0.000
	C2C	0.076	0.090
	C3C	−0.164	−0.313
	C4C	−0.084	−0.043
	C1D	−0.292	−0.345
	C2D	0.199	0.191
	C3D	−0.335	−0.324
	C4D	0.051	0.020
	CHA	−0.193	−0.187
	HA	0.211	0.200
	CHB	−0.248	−0.316
	HB	0.214	0.228
	CHC	−0.179	−0.185
	HC	0.176	0.165
	CHD	−0.012	−0.018
	HD	0.177	0.173
	CMA	−0.331	−0.211
	HMA1	0.141	0.095
	HMA2	0.141	0.095
	HMA3	0.141	0.095
	CAA	0.241	0.169
	HAA1	−0.004	−0.003
	HAA2	−0.004	−0.003
	CMB	−0.374	−0.314
	HMB1	0.139	0.110
	HMB2	0.140	0.110
	HMB3	0.139	0.110
	CAB	0.344	0.404
	HAB1	0.014	−0.001
	CBB	−0.359	−0.366
	HXB1	0.108	0.098
	HXB2	0.108	0.098
	HXB3	0.108	0.099

Table 1.3 continued

atom		partial charge	
		ox	red
haem	CMC	−0.443	−0.378
	HMC1	0.149	0.116
	HMC2	0.150	0.116
	HMC3	0.149	0.116
	CAC	0.324	0.504
	HAC1	−0.013	−0.067
	CBC	−0.295	−0.332
	HYC1	0.104	0.094
	HYC2	0.105	0.095
	HYC3	0.105	0.095
	CMD	−0.498	−0.463
	HMD1	0.172	0.148
	HMD2	0.172	0.148
	HMD3	0.172	0.149
	CAD	0.221	0.168
	HAD1	0.005	0.003
	HAD2	0.005	0.003
Cys101	SG	−0.286	−0.347
	CB	−0.005	−0.002
	HB1	0.060	0.060
	HB2	0.060	0.059
Cys104	SG	−0.343	−0.436
	CT2	0.355	0.319
	HB1	−0.087	−0.072
	HB2	−0.087	−0.072
His105	CB	0.206	0.133
	HB1	0.010	0.014
	HB2	0.010	0.014
	ND1	−0.243	−0.300
	HD1	0.364	0.357
	CG	−0.084	−0.021
	NE2	−0.171	−0.196
	CD2	−0.242	−0.275
	HD2	0.215	0.208
	CE1	−0.073	−0.053
	HE1	0.167	0.149
Met225	CB	0.031	−0.063
	HB1	0.009	0.027
	HB2	0.009	0.027
	CG	0.120	0.196
	HG1	0.002	−0.026
	HG2	0.002	−0.026
	SD	−0.227	−0.308
	CE	−0.109	−0.094
	HE1	0.076	0.057
	HE2	0.076	0.057
	HE3	0.077	0.058

Table 1.4a. Partial charges in e for the oxidised Rieske cluster in protonation forms P (both ligand histidines protonated), D1 (His161 deprotonated), D2 (His181 deprotonated), DT (both histidines deprotonated).

atom		partial charge			
		P	D1	D2	DT
$[Fe_2S_2]$	FE1	0.537	0.616	0.616	0.694
	FE2	0.503	0.589	0.564	0.662
	S1	−0.323	−0.367	−0.372	−0.422
	S2	−0.360	−0.431	−0.396	−0.473
His161	N	−0.576	−0.527	−0.579	−0.503
	CA	0.306	0.259	0.329	0.228
	C	0.430	0.429	0.419	0.461
	O	−0.519	−0.516	−0.528	−0.533
	CB	−0.116	−0.016	−0.061	0.076
	CG	0.020	−0.213	−0.001	−0.257
	ND1	−0.184	−0.227	−0.190	−0.229
	CD2	−0.229	0.038	−0.251	0.030
	CE1	−0.035	0.090	0.006	0.123
	NE2	−0.241	−0.500	−0.256	−0.540
	HN	0.286	0.272	0.299	0.275
	HA	0.064	0.073	0.047	0.066
	HB1	0.047	0.040	0.014	−0.001
	HB2	0.079	0.031	0.059	0.003
	HD2	0.234	0.129	0.221	0.111
	HE1	0.134	0.088	0.131	0.102
	HE2	0.385	0.000	0.375	0.000
His181	N	−0.507	−0.442	−0.481	−0.459
	CA	0.443	0.404	0.509	0.481
	C	0.389	0.367	0.316	0.300
	O	−0.440	−0.446	−0.456	−0.466
	CB	−0.357	−0.300	−0.242	−0.201
	CG	0.377	0.361	0.121	0.101
	ND1	−0.181	−0.243	−0.280	−0.341
	CD2	−0.421	−0.376	−0.077	−0.032
	CE1	−0.191	−0.156	0.066	0.085
	NE2	−0.103	−0.135	−0.469	−0.519
	HN	0.137	0.098	0.125	0.099
	HA	−0.001	−0.006	−0.027	−0.035
	HB1	0.104	0.094	0.044	0.034
	HB2	0.083	0.081	0.062	0.069
	HD2	0.285	0.260	0.156	0.131
	HE1	0.222	0.216	0.122	0.119
	HE2	0.355	0.346	0.000	0.000

Table 1.4a continued

atom		partial charge			
		P	D1	D2	DT
Cys159	CB	0.260	0.198	0.194	0.134
	SG	−0.427	−0.467	−0.482	−0.508
	HB1	−0.051	−0.047	−0.048	−0.043
	HB2	−0.045	−0.037	−0.035	−0.028
Cys178	CB	0.219	0.156	0.173	0.105
	SG	−0.407	−0.477	−0.461	−0.514
	HB1	−0.035	−0.028	−0.033	−0.023
	HB2	−0.025	−0.013	−0.025	−0.012
Thr160	C	0.471	0.409	0.438	0.369
	O	−0.501	−0.509	−0.513	−0.519
Leu162	N	−0.434	−0.384	−0.393	−0.396
	HN	0.203	0.190	0.175	0.189
	CA	0.163	0.127	0.171	0.148
	HA	0.049	0.036	0.027	0.012
Cys180	N	−0.485	−0.486	−0.505	−0.506
	HN	0.278	0.294	0.294	0.307
	CA	0.135	0.119	0.135	0.133
	HA	0.069	0.066	0.075	0.062
	C	0.429	0.454	0.427	0.482
	O	−0.465	−0.499	−0.465	−0.501
Pro179	C	0.457	0.415	0.409	0.370
	O	−0.494	−0.496	−0.493	−0.499

Table 1.4b. Partial charges in e for the reduced Rieske cluster in protonation forms P (both ligand histidines protonated), D1 (His161 deprotonated), D2 (His181 deprotonated). The reducing electron is formally placed at the histidine-coordinated iron atom [4].

atom		partial charge		
		P	D1	D2
$[Fe_2S_2]$	FE1	0.727	0.777	0.775
	FE2	0.387	0.508	0.474
	S1	−0.470	−0.516	−0.529
	S2	−0.522	−0.590	−0.557
His161	N	−0.582	−0.496	−0.573
	CA	0.335	0.189	0.312
	C	0.404	0.454	0.438
	O	−0.539	−0.542	−0.556
	CB	−0.032	0.105	0.068
	CG	−0.025	−0.281	−0.081
	ND1	−0.126	−0.178	−0.118
	CD2	−0.259	0.025	−0.265
	CE1	−0.072	0.069	−0.022
	NE2	−0.245	−0.565	−0.272
	HN	0.306	0.283	0.310
	HA	0.047	0.081	0.039
	HB1	0.002	−0.006	−0.039
	HB2	0.048	−0.008	0.017
	HD2	0.216	0.100	0.199
	HE1	0.129	0.079	0.133
	HE2	0.364	0.000	0.354
His181	N	−0.422	−0.393	−0.459
	CA	0.411	0.385	0.483
	C	0.363	0.346	0.306
	O	−0.469	−0.483	−0.491
	CB	−0.198	−0.189	−0.114
	CG	0.247	0.287	0.026
	ND1	−0.124	−0.242	−0.256
	CD2	−0.387	−0.353	−0.080
	CE1	−0.201	−0.144	0.052
	NE2	−0.166	−0.200	−0.543
	HN	0.090	0.070	0.116
	HA	−0.018	−0.025	−0.039
	HB1	0.047	0.048	−0.006
	HB2	0.064	0.070	0.046
	HD2	0.257	0.232	0.132
	HE1	0.210	0.202	0.112
	HE2	0.345	0.332	0.000

Table 1.4b continued

atom		partial charge		
		P	D1	D2
Cys159	CB	0.152	0.102	0.079
	SG	−0.527	−0.545	−0.551
	HB1	−0.045	−0.041	−0.036
	HB2	−0.024	−0.022	−0.010
Cys178	CB	0.130	0.065	0.072
	SG	−0.522	−0.562	−0.553
	HB1	−0.029	−0.015	−0.016
	HB2	−0.012	−0.004	−0.013
Thr160	C	0.432	0.364	0.401
	O	−0.521	−0.529	−0.533
Leu162	N	−0.353	−0.359	−0.345
	HN	0.177	0.198	0.152
	CA	0.135	0.112	0.150
	HA	0.028	0.013	0.005
Cys180	N	−0.478	−0.476	−0.480
	HN	0.298	0.308	0.298
	CA	0.104	0.098	0.090
	HA	0.065	0.056	0.072
	C	0.443	0.481	0.472
	O	−0.494	−0.531	−0.502
Pro179	C	0.407	0.369	0.365
	O	−0.508	−0.512	−0.509

Table 1.5. Partial charges in e for coenzyme Q with a tail of one isopren unit in its oxidised and deprotonated quinone (Q) and reduced and protonated quinol (QH_2) form. The partial charges of the additional five isopren units (not listed) of the CoQ molecule in the Q_i-site are set to zero.

atom	partial charge	
	Q	QH_2
C5	0.36837	0.14925
O5	−0.35301	−0.41856
HO5	—	0.36195
C4	0.10349	−0.04117
O4	−0.16794	−0.15752
C4M	−0.20052	−0.07522
H4M1	0.14100	0.10861
H4M2	0.10800	0.06012
H4M3	0.12024	0.06285
C3	−0.09075	0.23368
O3	−0.19273	−0.28429
C3M	−0.11284	0.02968
H3M1	0.09290	0.01456
H3M2	0.07767	0.03083
H3M3	0.12781	0.10030
C2	0.42045	−0.00185
O2	−0.37632	−0.42853
HO2	—	0.37599
C1	−0.01112	−0.02319
C1M	−0.26143	−0.11868
H1M1	0.10440	0.05834
H1M2	0.11162	0.07540
H1M3	0.10714	0.05672
C6	−0.37103	−0.43849
C7	0.44735	0.49081
C8	−0.43250	−0.44351
C9	0.19036	0.17942
C10	−0.46670	−0.47080
C11	−0.33664	−0.30167
HA7	−0.02862	−0.05650
HB7	−0.01686	−0.00246
H8	0.16233	0.15614
HA10	0.11729	0.10775
HB10	0.10224	0.09612
HC10	0.09726	0.08386
HA11	0.20955	0.21503
HB11	0.20954	0.21503
HC11	0.00000	0.00000

Table 1.6. Partial charges in e for stigmatellin. Partial charges of the hydrophobic part of the tail (not listed) have been set to zero.

atom	partial charge
O1	−0.169
C2	−0.029
C3	−0.132
C3M	−0.350
C4	0.548
O4	−0.472
C4A	−0.447
C5	0.349
O5	−0.171
C5M	−0.136
C6	−0.500
C7	0.318
O7	−0.128
C7M	−0.272
C8	−0.105
O8	−0.450
C8A	0.226
C9	0.196
H3M1	0.127
H6	0.232
H3M2	0.137
H3M3	0.129
H5M1	0.128
H5M2	0.077
H5M3	0.078
H7M1	0.164
H7M2	0.113
H7M3	0.123
H8	0.408
H91	0.000
H92	0.009

Table 1.6 continued

atom	partial charge
C10	−0.035
C11	0.250
C22	−0.485
C12	0.257
O12	−0.407
C23	0.078
C13	0.035
C24	−0.375
C14	0.139
O14	−0.282
C25	−0.185
C15	0.035
H101	0.004
H103	−0.015
H11	−0.017
H221	0.126
H222	0.123
H223	0.119
H12	−0.046
H231	0.071
H232	0.008
H233	0.005
H13	0.007
H241	0.124
H242	0.084
H243	0.081
H14	0.038
H251	0.120
H252	0.086
H253	0.079
H15	−0.023

Table 1.7. Partial charges in e for undecylstigmatellin in its oxidised and reduced form.

atom	partial charge	
	ox	red
O1	0.006098	−0.022465
C2	−0.063771	−0.091201
C3	−0.026548	−0.143828
C3M	−0.318529	−0.311142
C4	0.293678	0.340300
O4	−0.422153	−0.503714
C4A	−0.000620	0.027629
C5	0.006310	−0.141215
O5	−0.106671	−0.141544
C5M	−0.105531	−0.059191
C6	−0.189797	−0.136481
C7	0.019246	−0.013586
O7	−0.108347	−0.115356
C7M	−0.154056	−0.146444
C8	0.190583	0.203661
O8	−0.469020	−0.463242
C8A	−0.208825	−0.240480
C9	0.007485	0.100498
H3M1	0.106535	0.117818
H3M2	0.137295	0.126583
H3M3	0.126629	0.102474
H5M1	0.111068	0.083988
H5M2	0.083289	0.070543
H5M3	0.080450	0.066848
H6	0.148978	0.164488
H41	—	0.048190
H7M1	0.124448	0.129902
H7M2	0.098467	0.086265
H7M3	0.100673	0.090700
H8	0.384553	0.386562
H42	0.025618	0.324141
H91	0.055456	0.003180
H92	—	0.033810

Table 1.7 continued

atom	partial charge	
	ox	red
C10	0.085321	−0.003879
C11	−0.067355	−0.032991
C12	−0.037340	−0.052403
C13	0.055739	0.049039
C14	−0.107655	−0.109430
C15	0.062102	0.065836
C16	−0.077202	−0.074198
C17	−0.066264	−0.073395
C18	0.164461	0.157065
C19	−0.331357	−0.329418
H101	−0.002045	0.011603
H102	−0.021128	−0.005753
H111	0.029361	0.029299
H112	0.023253	0.015414
H121	0.020517	0.024056
H122	0.017599	0.018354
H131	−0.010298	−0.004366
H132	−0.001366	0.001650
H141	0.023377	0.026012
H142	0.022704	0.020376
H151	−0.005278	−0.006641
H152	−0.007517	−0.009149
H161	0.033860	0.035908
H162	0.019642	0.015608
H171	0.017567	0.021575
H172	0.024020	0.028660
H181	−0.019603	−0.020786
H182	−0.028316	−0.025206
H191	0.092180	0.086345
H192	0.079661	0.078755
H193	0.078369	0.084369

Table 1.8. Partial charges in e for the headgroup of hydroxydioxobenzothiazole in its protonated and deprotonated form. Partial charges of the hydrophobic tail (not listed) have been set to zero.

atom	partial charge	
	prot	deprot
S1	0.122	0.004
C7A	−0.263	−0.169
C4A	0.200	0.238
N3	−0.370	−0.384
C2	0.014	−0.051
H2	0.204	0.175
C4	0.412	0.218
O4	−0.379	−0.467
C5	−0.325	−0.256
C6	0.084	0.160
C7	0.466	0.376
O7	−0.342	−0.419
O6	−0.442	−0.481
HO6	0.434	− − −
C8	0.102	0.059
HA8	0.018	0.001
HB8	0.065	−0.004

Table 1.9. Partial charges in e for the head group of phosphatidylethanolamine in its three protonation forms (prot: doubly protonated, deprotN: deprotonated at amine group, deprotP: deprotonated at phosphate group). Charges of atoms in the hydrophobic tails (not listed) are set to zero.

atom	partial charge		
	prot	deprotN	deprotP
C5	0.399	0.051	0.051
N	−0.559	−0.821	−0.821
HN3	0.364	0.000	0.000
HN1	0.377	0.320	0.320
HN2	0.377	0.320	0.320
HA5	0.021	0.065	0.065
HB5	0.021	0.065	0.065
C1	0.302	0.302	0.113
C4	0.291	0.291	0.107
O3P	−0.374	−0.374	−0.415
O1P	−0.302	−0.302	−0.687
O2P	−0.317	−0.317	−0.686
O4P	−0.344	−0.344	−0.410
P	0.753	0.753	0.949
HA1	−0.003	−0.003	0.017
HB1	−0.003	−0.003	−0.003
HA4	0.008	0.008	0.021
HB4	−0.011	−0.011	−0.006
C10	0.649	0.649	0.649
C11	−0.258	−0.258	−0.258
C12	0.025	0.025	0.025
C2	0.239	0.239	0.239
O4	−0.476	−0.476	−0.476
O2	−0.438	−0.438	−0.438
HA11	0.094	0.094	0.094
HB11	0.088	0.088	0.088
HA12	0.028	0.028	0.028
HB12	0.010	0.010	0.010
H2	0.039	0.039	0.039
C30	0.586	0.586	0.586
C31	−0.216	−0.216	−0.216
C32	0.062	0.062	0.062
C3	0.308	0.308	0.308
O5	−0.478	−0.478	−0.478
O3	−0.424	−0.424	−0.424
HA31	0.083	0.083	0.083
HB31	0.083	0.083	0.083
HA32	0.004	0.004	0.004
HB32	0.004	0.004	0.004
HA3	−0.006	−0.006	−0.006
HB3	−0.006	−0.006	−0.006

Table 1.10. Partial charges in e for the head group of phosphatic acid in its two protonation forms (prot: singly protonated phosphate group with net charge of -1, deprot: deprotonated phosphate group with net charge of -2). Charges of atoms in the hydrophobic tails (not listed) are set to zero.

atom	partial charge	
	prot	deprot
P	1.007	−0.360
O11	−0.406	−0.095
O12	−0.510	−0.492
O13	−0.511	−0.436
O14	−0.689	−0.440
C1	0.083	−0.327
H11	−0.001	0.086
H12	0.027	0.064
C2	0.239	0.239
H2	0.039	0.039
O21	−0.438	−0.438
O22	−0.476	−0.476
C21	0.649	0.649
C22	−0.258	−0.258
H221	0.094	0.094
H222	0.088	0.088
C23	0.025	0.025
H231	0.028	0.028
H232	0.010	0.010

Table 1.11. Partial charges in e for the phosphodiester moieties in the head group of cardiolipin in their two protonation forms (prot: protonated phosphodiester with net charge 0, deprot: deprotonated phospodiester with net charge −1). Charges of atoms in the hydrophobic tails (not listed) are set to zero.

atom	partial charge	
	prot	deprot
C1	0.243	0.243
O1	−0.553	−0.553
H1	−0.022	−0.022
HO1	0.332	0.332
CA2	0.302	0.113
OA2	−0.374	−0.415
PA1	0.753	0.949
OA4	−0.506	−0.686
OA3	−0.521	−0.687
OA5	−0.344	−0.410
CA3	0.291	0.107
HAA2	−0.003	0.007
HBA2	−0.003	0.007
HAA3	0.008	0.007
HBA3	−0.011	0.008
CB2	0.302	0.302
OB2	−0.374	−0.374
PB2	0.753	0.753
OB4	−0.506	−0.506
OB3	−0.521	−0.521
OB5	−0.344	−0.344
CB3	0.291	0.291
HAB2	−0.003	−0.003
HBB2	−0.003	−0.003
HAB3	0.008	0.008
HBB3	−0.011	−0.011
CB7	0.586	0.586
OB9	−0.478	−0.478
OB8	−0.424	−0.424
C71	−0.216	−0.216
C72	0.062	0.062
HA71	0.083	0.083
HB71	0.083	0.083
HA72	0.004	0.004
HB72	0.004	0.004

Table 1.11 continued

atom	partial charge	
	prot	deprot
CB6	0.308	0.308
HAB6	−0.006	−0.006
HBB6	−0.006	−0.006
CA7	0.586	0.586
OA9	−0.478	−0.478
OA8	−0.424	−0.424
C31	−0.216	−0.216
C32	0.062	0.062
HA31	0.083	0.083
HB31	0.083	0.083
HA32	0.004	0.004
HB32	0.004	0.004
CA6	0.308	0.308
HAA6	−0.006	−0.006
HBA6	−0.006	−0.006

Table 1.12. Partial charges in e for the head group of the phosphatidylcholin in its two protonation forms. Charges for the cholin moiety are taken from the CHARMM27 parameter set. Charges of atoms in the hydrophobic tails (not listed) are set to zero.

atom	partial charge	
	prot	deprot
N	−0.600	−0.600
C12	−0.100	−0.100
C13	−0.350	−0.350
C14	−0.350	−0.350
C15	−0.350	−0.350
HA12	0.250	0.250
HB12	0.250	0.250
HA13	0.250	0.250
HB13	0.250	0.250
HC13	0.250	0.250
HA14	0.250	0.250
HB14	0.250	0.250
HC14	0.250	0.250
HA15	0.250	0.250
HB15	0.250	0.250
HC15	0.250	0.250
C11	0.302	0.113
C1	0.291	0.107
O13	−0.374	−0.415
O12	−0.506	−0.687
O14	−0.521	−0.686
O11	−0.344	−0.419
P	0.753	0.949
HA11	−0.003	0.017
HB11	−0.003	−0.003
HO	0.408	0.000
HA1	0.008	0.021
HB1	−0.011	−0.006
C21	0.649	0.649
O22	−0.476	−0.476
O21	−0.438	−0.438
C22	−0.258	−0.258
C23	0.025	0.025
HA22	0.094	0.094
HB22	0.088	0.088
HA23	0.028	0.028
HB23	0.010	0.010
C2	0.239	0.239
H2	0.039	0.039

Table 1.12 continued

atom	partial charge	
	prot	deprot
C31	0.586	0.586
O32	−0.478	−0.478
O31	−0.424	−0.424
C32	−0.216	−0.216
C33	0.062	0.062
HA32	0.083	0.083
HB32	0.083	0.083
HA33	0.004	0.004
HB33	0.004	0.004
C3	0.308	0.308
HA3	−0.006	−0.006
HB3	−0.006	−0.006

Table 1.13. Partial charges in e for the head group of the phosphatidylinositol in its two protonation forms. Charges of atoms in the hydrophobic tails (not listed) are set to zero.

atom	partial charge	
	prot	deprot
P	1.141	1.064
O11	−0.444	−0.397
O12	−0.566	−0.702
O13	−0.569	−0.689
O14	−0.443	−0.447
C5’	0.448	0.260
C6’	0.383	0.431
C1’	0.057	0.058
C2’	0.342	0.432
C3’	0.143	0.376
C4’	−0.001	0.000
O6’	−0.679	−0.659
O1’	−0.638	−0.661
O2’	−0.636	−0.693
O3’	−0.598	−0.684
O4’	−0.597	−0.599
C1	0.179	0.122
H5’	−0.065	0.012
H6’	−0.019	−0.053
H1’	0.028	−0.022
H2’	−0.025	−0.047
H3’	−0.015	−0.113
H4’	0.036	0.034
HO6	0.435	0.397
HO1	0.437	0.435
HO2	0.395	0.393
HO3	0.412	0.412
HO4	0.397	0.348
H13	0.400	0.000
H1A	0.059	0.004
H1B	0.003	−0.012
C21	0.586	0.586
O22	−0.478	−0.478
O21	−0.424	−0.424

Table 1.13 continued

atom	partial charge	
	prot	deprot
C22	−0.216	−0.216
C23	0.062	0.062
HA22	0.083	0.083
HB22	0.083	0.083
HA23	0.004	0.004
HB23	0.004	0.004
C2	0.308	0.308
HA2	−0.006	−0.006
HB2	−0.006	−0.006
C31	0.649	0.649
O32	−0.476	−0.476
O31	−0.438	−0.438
C32	−0.258	−0.258
C33	0.025	0.025
HA32	0.094	0.094
HB32	0.088	0.088
HA33	0.028	0.028
HB33	0.010	0.010
C3	0.239	0.239
H3	0.039	0.039

Table 1.14. Partial charges in e for the head group of the detergent undecylmaltopyranoside. Charges of atoms in the hydrophobic tail (not listed) are set to zero.

atom	partial charge
C1	0.200
H1	0.090
O1	−0.520
C5	0.250
H5	0.090
O5	−0.400
C2	0.140
H2	0.090
O2	−0.660
HO2	0.430
C3	0.140
H3	0.090
O3	−0.660
HO3	0.430
C4	0.140
H4	0.090
O4	−0.660
HO4	0.430
C6	0.050
H61	0.090
H62	0.090
O6	−0.660
HO6	0.430

Table 1.14 continued

atom	partial charge
C4'	0.200
H4'	0.090
C6'	0.050
H61'	0.090
H62'	0.090
O6'	−0.660
H'O6	0.430
C2'	0.140
H2'	0.090
O2'	−0.660
H'O2	0.430
C3'	0.140
H3'	0.090
O3'	−0.660
H'O3	0.430
C1'	0.200
H1'	0.090
O1'	−0.430
C5'	0.250
H5'	0.090
O5'	−0.400
CA	0.100
HA1	0.050
HA2	0.050

2. Calculation of relative energies of the two Q_o-site conformations

The crystal structures of cytochrome bc_1 from *S. cerevisiae* [2, 3, 15, 16] reveal two alternative conformations of the Q_o-site. The most obvious difference is the orientation of the sidechain of Glu272 of the cytochrome *b* subunit. In the structure containing stigmatellin, Glu272 is oriented towards the inhibitor and the Rieske iron-sulphur cluster (conformation Glu-FeS). In the structure containing hydroxydioxobenzothiazole (HDBT), it is oriented away from the inhibitor and towards haem b_L (conformation Glu-*b*). To include the conformational flexibility of the Q_o-site into Poisson-Boltzmann (PB)/Monte Carlo titration calculations, the energy difference between the two conformations needs to be calculated.

By visual inspection of the two crystal structures a fragment of the cytochrome *b* subunit could be identified that contains all residues undergoing significant conformational changes, namely residues Thr265 to Trp273 and the sidechain of His253. The energy of this fragment in the two different conformations in the environment of completely reduced or oxidised cytochrome bc_1 has been calculated by a combined molecular mechanics (MM)/PB-approach.

The conformational energy has two contributions (Fig. 2):

$$\Delta G_{\rm conf} = \Delta G_{\rm MM} + \Delta\Delta G_{\rm PB}\,.$$

$\Delta G_{\rm MM} = G_{\rm MM}(\text{Glu-FeS}) - G_{\rm MM}(\text{Glu-}b)$ is the difference in the MM energy of the fragment in the two conformations. This MM contribution was calculated using CHARMM [1]: the fragment in conformations Glu-FeS or Glu-*b* was placed into a homogeneous dielectric environment (dielectric constant $\epsilon = 4$, Fig. 2), and the relevant contributions to the MM energy were calculated. These contributions are the energies of the dihedral angles, the van der Waals interaction energies of atoms connected by three covalent bonds, and the electrostatic interaction energies of atoms that are separated by three or more covalent bonds, as implemented in the CHARMM energy function. The difference in the dihedral, van der Waals and electrostatic energies of the fragment in conformation Glu-FeS and conformation Glu-*b* is equivalent to $\Delta G_{\rm MM}$.

In addition to the difference in MM energies in a homogeneous environment, the electrostatics of the protein/membrane environment can also exert differential effects on the fragment

Figure 2. Calculation of the energy difference $\Delta G_{\rm conf}$ of the Glu-FeS and Glu-*b* conformations of the Q_o-site of membrane-embedded cytochrome bc_1.

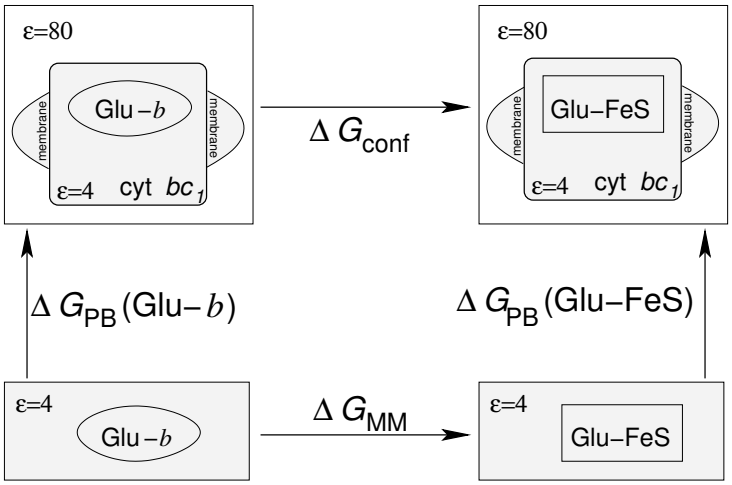

Table 2. Results from the calculation of the conformational energy difference between the Glu-*b* and Glu-FeS conformations of the Q_o-site of completely oxidised and reduced cytochrome bc_1 in presence of a model membrane. All energies are in kcal/mol.

energy contribution	oxidised system		reduced system	
	Glu-FeS	Glu-*b*	Glu-FeS	Glu-*b*
CHARMM van der Waals energies	59.3	54.3	59.2	54.3
CHARMM electrostatic energies	60.5	62.0	60.5	62.1
CHARMM dihedral energies	94.8	95.3	94.6	95.0
sum of CHARMM energies G_{MM}	214.6	211.6	214.3	211.4
MEAD transfer energies ΔG_{PB}	−48.7	−55.1	−52.4	−60.2
resulting $G^{\mathrm{conf}} = G_{\mathrm{MM}} + \Delta G_{\mathrm{PB}}$	165.9	156.6	161.9	151.2
resulting $\Delta G^{\mathrm{conf}} = \Delta G_{\mathrm{MM}} + \Delta\Delta G_{\mathrm{PB}}$	9.4		10.7	

in the two different conformations. This effect of the protein/membrane environment is quantified by PB-calculations: the energy ΔG_{PB} to transfer the fragment from the homogeneous environment of the MM-calculations into the protein environment (Fig. 2) is calculated with MEAD [17], once for the Glu-*b* conformation and once for the Glu-FeS conformation.

The crystal structure obtained with HDBT has been used as protein environment for the Q_o-site fragment in both the Glu-FeS and Glu-*b* conformations since the HDBT-inhibited structure contains additionally refined lipids. Differences between the HDBT- and stigmatellin-inhibited structures are limited to the Q_o-site fragments treated in the MM calculations. The interface between the protein environment and the Q_o-site fragment in the Glu-FeS conformation was very mildly energy minimised before the calculation of conformational energies and the MEAD calculations. The minimisation consisted of 1000 steepest decent (SD) steps, 500 molecular dynamics (MD) steps of 0.2 fs at $100\,K$, 500 MD steps of 0.5 fs at $200\,K$, 500 MD steps of 0.1 fs at $300\,K$, 500 MD steps of 0.1 fs at $100\,K$, 1000 SD steps and 2000 conjugate gradient steps. Only atoms directly at the interface and atoms that are connected to the interface atoms by one covalent bond were allowed to move. The rmsd between the structures before and after minimisation is as low as 0.11 Å. In the protein environment, the protein atoms carry charges (the protonation state is set to be the doubly protonated form for the histidines, and the neutral form for all other residues), and the dielectric environment is not homogeneous. In the PB-calculations, the charges of the C_α atoms located directly at the interface of the Q_o-site fragments and the protein environment, i.e. the C_α atoms of His253, Val264 and Trp273, were set to zero in order to eliminate unphysical coulombic interaction between atoms connected by covalent bonds.

From the difference in the Poisson-Boltzmann energies ($\Delta\Delta G_{\mathrm{PB}}$) together with the difference in MM energy (ΔG_{MM}), the conformational energy difference in the protein environment (ΔG_{conf}) can be obtained. Table 2 lists results obtained for the different quantities.

3. Model compound pK-values for Poisson-Boltzmann calculations

In the framework of PB electrostatics, the energetics of a system with multiple titratable groups can be described by a set of intrinsic pK-values and pairwise interaction energies. The intrinsic pK-value of a certain group is the pK-value the group would have if all other titratable groups in the system were in a certain reference protonation form. By the programme multiflex from the MEAD programme suite [17] intrinsic pK-values are computed as shifts relative to model compound pK-values. The model pK-value of a certain group corresponds to the pK-value it would have as an isolated group in aqueous solution. Table 3 lists experimentally determined model pK-values [18, 19] that have been used in this work. Model compound pK-values for the Rieske ligand histidines have been determined by a combined DFT/PB approach described below.

Table 3. Groups in cytochrome bc_1 considered titratable, and corresponding experimentally determined model compound pK-values [18, 19].

group	model pK-value
arginine	12.0
lysine	10.4
tyrosine	9.6
cysteine	9.1
histidine NδH	6.6
histidine NϵH	7.0
aspartate	4.0
glutamate	4.4
N-terminus	7.5
C-terminus	3.8
haem propionate	4.4
lipid phosphodiester	1.3
phosphatic acid phosphate	6.3
phosphatidyl ethanolamine	10.6

4. Calculation of model compound pK-values for the Rieske cluster

For the Rieske iron-sulphur cluster with its titratable ligand histidine sidechains, experimentally determined model pK-values are not available. We have therefore estimated these values from a combined DFT/PB approach that makes use of the thermodynamic cycle depicted in Fig. 4.

The deprotonation energies of the Rieske cluster in vacuum are known from DFT calculations that have been reported earlier, and could be shown to reproduce experimental results in combined DFT/PB calculations [5, 20]. The model compound is defined to contain the same set of atoms that is included into these DFT calculations. The energies to transfer the protonated and deprotonated species ($\Delta G_{\mathrm{trans}}(\mathrm{AH})$ and $\Delta G_{\mathrm{trans}}(\mathrm{A}^-)$, respectively) from vacuum ($\epsilon = 1$) into the aqueous environment ($\epsilon = 80$) are obtained from PB electrostatics calculations using solvate from the MEAD package. The ionic strength is set to $I = 0.1\,\mathrm{M}$ in these calculations, the temperature to $T = 300\,\mathrm{K}$. The transfer energy of the proton is calculated from the experimentally derived potential of the standard hydrogen electrode [21]. The model compound pK-values were calculated as

$$\mathrm{p}K^{\mathrm{model}} = (\ln 10 \cdot RT)^{-1} \Delta G^{\mathrm{aq}}_{\mathrm{deprot}}$$

with R as universal gas constant and

$$\Delta G^{\mathrm{aq}}_{\mathrm{deprot}} = \Delta G^{\mathrm{vac}}_{\mathrm{deprot}} + \Delta G_{\mathrm{trans}}(\mathrm{A}^-) + \Delta G_{\mathrm{trans}}(\mathrm{H}^+) - \Delta G_{\mathrm{trans}}(\mathrm{AH})\,.$$

The procedure was followed for all considered one-proton deprotonation reactions of the Rieske cluster in its different redox states. Resulting model compound pK-values are listed in Table 4.

Figure 4. Thermodynamic cycle to obtain the model pK-values of the Rieske cluster as isolated group in aqueous solution. AH represents the protonated, and A^- the deprotonated form of the Rieske cluster.

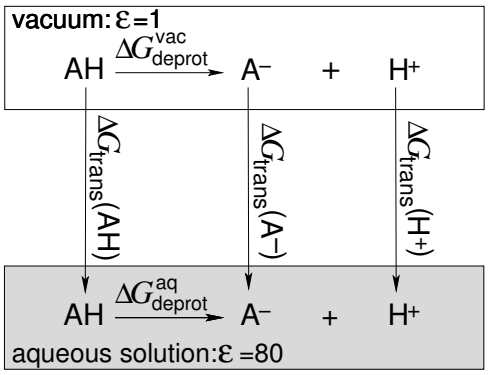

Table 4. Model compound pK-values for the ligand histidines of the Rieske centre. The following protonation forms have been considered: both ligand histidines protonated (P), only H161 deprotonated (D1), only H181 deprotonated (D2), both ligand histidines deprotonated (DT, considered only in the oxidised state).

redox state	deprotonation reaction	model pK-value
oxidized	P$\longrightarrow$D1	9.1
	P$\longrightarrow$D2	8.8
	D1$\longrightarrow$DT	8.6
	D2$\longrightarrow$DT	9.0
reduced	P$\longrightarrow$D1	10.6
	P$\longrightarrow$D2	12.4

5. Treatment of the Rieske cluster in MEAD calculations

The Rieske iron-sulphur cluster has two histidine ligands that can potentially undergo (de)protonation reactions. The Rieske cluster therefore has four different protonation forms: both histidines protonated (P), only $H161^{ISP}$ deprotonated (D1), only $H181^{ISP}$ deprotonated (D2), or both histidines deprotonated (DT). In the following, we focus on the situation of the oxidised cluster, where all four possible protonation forms have been considered. The treatment of the reduced cluster is equivalent but more simple, since the doubly deprotonated form does not need to be considered due to its low probability at physiological pH [4, 5].

The multiflex titration programme from the MEAD programme suite only considers conversions between exactly two different forms of a titratable group. Therefore, four separate multiflex calculations were run for the oxidised state of the system, referred to as P→D1, P→D2, D1→DT and D2→DT in analogy to the different possible deprotonation reactions of the Rieske cluster. The separate multiflex calculations are however not sufficient to decide upon the protonation form of the Rieske cluster in the protein, since the different protonation reactions influence the energetics of each other. These interactions are not accounted for by multiflex calculations considering only a single one-proton deprotonation reaction at a time. An approach based on Monte Carlo (MC) sampling of state energies was thus used in this study, and is outlined in the following.

To fully characterise the protonation behaviour of the Rieske cluster, the multiflex calculations listed above are treated like different conformations of a protein. The four different one-proton titration reactions of the oxidised Rieske cluster are assigned relative 'conformational' energies. In the reference state, for which the conformational energies are computed (named 'MC reference state' in the following), the Rieske cluster is in its protonated form, the histidines are protonated, and all other residues are in their neutral protonation form. The fact that the Rieske cluster is in its protonated form in the MC reference state means that the conformational energies have to be computed for the Rieske cluster being in its P form for the P→D1 and P→D2-titrations, in its D1 form for the D1→DT titration, and in its D2 form for the D2→DT titration (see Table 5). Thus, the relative 'conformational' energies are in fact differences in protonation state energies.

Table 5. The MC reference protonation state is defined to be the protonated form of the Rieske cluster for all four different multiflex calculations. Since different one-proton deprotonation reactions are considered in these multiflex calculations, the protonated form of the Rieske cluster has in fact different meanings in terms of the four possible protonation states of the Rieske cluster. The 'conformational' energy is thus a difference between the energies of the different protonation states that result from the definition of the MC reference state and the one-proton deprotonation reaction of the Rieske cluster considered in the respective multiflex calculation.

multiflex calculation:	P→D1	P→D2	D1→DT	D2→DT
Rieske protonation form in the MC reference state:	protonated	protonated	protonated	protonated
Rieske protonation form for which 'conformational' energy is computed:	P	P	D1	D2
'conformational' energy:	$\Delta G_{\mathrm{conf}}^{\mathrm{P}\rightarrow\mathrm{D1}}$	$\Delta G_{\mathrm{conf}}^{\mathrm{P}\rightarrow\mathrm{D2}}$	$\Delta G_{\mathrm{conf}}^{\mathrm{D1}\rightarrow\mathrm{DT}}$	$\Delta G_{\mathrm{conf}}^{\mathrm{D2}\rightarrow\mathrm{DT}}$

Figure 5. Calculation of $\Delta G_{\mathrm{conf}}^{\mathrm{D1}\rightarrow\mathrm{DT}}$ in a protein with two Rieske clusters, e.g. the dimeric form of the cytochrome bc_1 complex. $\Delta G_{\mathrm{conf}}^{\mathrm{D2}\rightarrow\mathrm{DT}}$ is computed analogously.

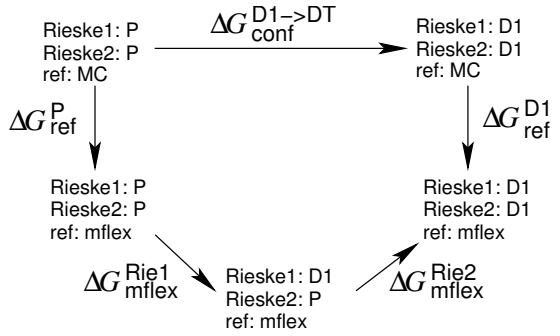

The differences in protonation state energies are computed relative to the energy assigned to the P→D1 multiflex calculation ($\Delta G_{\mathrm{conf}}^{\mathrm{P}\rightarrow\mathrm{D1}} = 0$). Since the MC reference state has identical meanings (Rieske cluster in its P form) for the P→D1 and P→D2 multiflex calculations, they have identical energies assigned ($\Delta G_{\mathrm{conf}}^{\mathrm{P}\rightarrow\mathrm{D1}} = \Delta G_{\mathrm{conf}}^{\mathrm{P}\rightarrow\mathrm{D12}} = 0$). According to Fig. 5, the 'conformational' energy $\Delta G_{\mathrm{conf}}^{\mathrm{D1}\rightarrow\mathrm{DT}}$ can be calculated as

$$\Delta G_{\mathrm{conf}}^{\mathrm{D1}\rightarrow\mathrm{DT}} = \Delta G_{\mathrm{mflex}}^{\mathrm{Rie1}} + \Delta G_{\mathrm{mflex}}^{\mathrm{Rie2}} + \left(\Delta G_{\mathrm{ref}}^{\mathrm{P}} - \Delta G_{\mathrm{ref}}^{\mathrm{D1}}\right) .$$

The four contributions can be obtained from the multiflex output (intrinsic pK-values and interaction energies). $\Delta G_{\mathrm{mflex}}^{\mathrm{Rie1}}$ can be calculated from the intrinsic pK of the first Rieske cluster in the P→D1 multiflex run:

$$\Delta G_{\mathrm{mflex}}^{\mathrm{Rie1}} = \ln 10 \cdot RT(\mathrm{p}K^{\mathrm{intr,P}\rightarrow\mathrm{D1}}(\mathrm{Rie1}) - \mathrm{pH}) .$$

$\Delta G_{\mathrm{mflex}}^{\mathrm{Rie2}}$ can be calculated from the intrinsic pK of the second Rieske cluster plus the interaction energy with the first Rieske cluster. The interaction energy has to be added, since the first Rieske cluster is then no longer in its reference state:

$$\Delta G_{\mathrm{mflex}}^{\mathrm{Rie2}} = \ln 10 \cdot RT(\mathrm{p}K^{\mathrm{intr,P}\rightarrow\mathrm{D1}}(\mathrm{Rie1}) - \mathrm{pH}) + W(\mathrm{Rie1}, \mathrm{Rie2}) .$$

The intrinsic pK-values are calculated for the multiflex reference protonation state (ref:mflex in Fig. 5), which is different from the MC reference state (ref:MC in Fig. 5). In order to derive $\Delta G_{\mathrm{conf}}^{\mathrm{D1}\rightarrow\mathrm{DT}}$ from $\Delta G_{\mathrm{mflex}}^{\mathrm{Rie1}}$ and $\Delta G_{\mathrm{mflex}}^{\mathrm{Rie2}}$, the pH-dependent energy differences $\Delta G_{\mathrm{ref}}^{\mathrm{D1}}$ and $\Delta G_{\mathrm{ref}}^{\mathrm{P}}$ between the MC and multiflex reference protonation states have to be considered. These energy differences are calculated directly from the protonation state energies $G^{(n)}$. The protonation state energies $G^{(n)}$ are computed from the multiflex intrinsic pK-values and interaction energies [18].

References

[1] A. D. MacKerell, D. Bashford, M. Bellott, R. L. Dunbrack jr, J. D. Evanseck, M. J. Field, S. Fischer, J. Gao, H. Guo, S. Ha, D. Joseph-McCarthy, L. Kuchnir, K. Kuczera, F. T. K. Lau, C. Mattos, S. Michnick, T. Ngo, D. T. Nguyen, B. Prodhom, W. E. Reiher, B. Roux, M. Schlenkrich, J. C. Smith, R. Stote, J. Straub, M. Watanabe, J. Wiorkiewicz-Kuczera, D. Yin, M. Karplus, All-atom empirical potential for molecular modeling and dynamics studies of proteins, J. Phys. Chem. B 102 (1998) 3586–3616.

[2] H. Palsdottir, C. G. Lojero, B. L. Trumpower, C. Hunte, Structure of the yeast cytochrome bc_1 with a hydroxyquinone anion Q_o site inhibitor bound, J. Biol. Chem. 278 (2003) 31303–31311.

[3] C. Lange, J. H. Nett, B. L. Trumpower, C. Hunte, Specific roles of protein-phospholipid interactions in the yeast cytochrome bc_1 complex structure, EMBO J. 20 (2001) 6591–6600.

[4] G. M. Ullmann, L. Noodleman, D. A. Case, Density functional calculation of the pK_a values and redox potentials in the bovine Rieske iron-sulfur protein, J. Biol. Inorg. Chem. 7 (2002) 632–639.

[5] A. R. Klingen, G. M. Ullmann, Negatively charged residues and hydrogen bonds tune the ligand histidine pK_a values of Rieske iron-sulfur proteins, Biochemistry 43 (2004) 12383–12389.

[6] B. Rabenstein, G. M. Ullmann, E.-W. Knapp, Energetics of electron-transfer and protonation reactions of the quinones in the photosynthetic reaction center of *Rhodopseudomonas viridis*, Biochemistry 37 (1998) 2488–2495.

[7] C. F. Guerra, J. G. Snijders, G. te Velde, E. J. Baerends, Towards an order-N DFT method, Theor. Chem. Acc. 99 (1998) 391–403.

[8] S. H. Vosko, L. Wilk, M. Nusair, Accurate spin-dependent electron liquid correlation energies for local spin density calculations: a critical analysis, Can. J. Phys. 58 (1980) 1200–1211.

[9] J. P. Perdew, J. A. Chevary, S. H. Vosko, K. A. Jackson, M. R. Pederson, D. J. Singh, C. Fiolhais, Atoms, molecules, solids, and surfaces: applications of the generalized gradient approximation for exchange and correlation, Phys. Rev. B 46 (1992) 6671–6687.

[10] C. M. Breneman, K. B. Wiberg, Determining atom-centered monopoles from molecular electrostatic potentials. The need for high spin sampling density in formamide conformational anlysis, J. Comput. Chem. 11 (1989) 361–373.

[11] J.-M. Mouesca, J. L. Chen, L. Noodleman, D. Bashford, D. A. Case, Density functional/Poisson-Boltzmann calculations of redox potentials for iron-sulfur clusters, J. Amer. Chem. Soc. 116 (1994) 11898–11914.

[12] A. Bondi, van der Waals volumes and radii, J. Phys. Chem. 68 (1964) 441–451.

[13] V. Konstanjevečki, D. Leys, G. Van Driessche, T. E. Meyer, M. A. Cusanovich, U. Fischer, Y. Guisez, J. Van Beeumen, Structure and Characterization of *Ectothiorhodospira vacuolata* cytochrome b_{558}, a prokaryotic homologue of cytochrome b_5, J. Biol. Chem. 274 (1999) 35614–35620.

[14] G. W. Bushnell, G. V. Louie, G. D. Brayer, High resolution three-dimensional structure of horse heart cytochrome c, J. Mol. Biol. 214 (1990) 585–595.

[15] C. Hunte, J. Koepke, C. Lange, T. Roßmanith, H. Michel, Structure at 2.3 Å of the cytochrome bc_1 complex from the yeast *Saccharomyces cerevisiae* co-crystallized with an antibody Fv fragment, Structure 8 (2000) 669–684.

[16] H. Palsdottir, C. Hunte, Lipids in membrane protein structures, Biochim. Biophys. Acta 1666 (2004) 2–18.

[17] D. Bashford, M. Karplus, pK_as of ionizable groups in proteins: atomic detail from a continuum electrostatic model, Biochemistry 29 (1990) 10219–10225.

[18] G. M. Ullmann, E.-W. Knapp, Electrostatic models for computing protonation and redox equilibria in proteins, Eur. Biophys. J. 28 (1999) 533–551.

[19] W. D. Kumler, J. J. Eiler, The acid strength of mono and diesters of phosphoric acid, J. Amer. Chem. Soc. 65 (1943) 2355–2361.

[20] G. M. Ullmann, The coupling of protonation and reduction in proteins with multiple redox centers: Theory, computational method, and application to cytochrome c_3, J. Phys. Chem. B 104 (2000) 6293–6301.

[21] H. Reiss, A. Heller, The absolute potential of the standard hydrogen electrode: a new estimate, J. Phys. Chem. 89 (1985) 4207–4213.